Inorganic Chemistry

Article

pubs.acs.org/IC

Zinc, Cadmium, and Mercury Complexes of a Pyridyloxy-Substituted Cyclotriphosphazene: Syntheses, Structures, and Fluxional Behavior

Eric W. Ainscough,* Andrew M. Brodie,* Patrick J. B. Edwards, Geoffrey B. Jameson, Carl A. Otter, and Stephen Kirk

Chemistry—Institute of Fundamental Sciences, Massey University, Private Bag 11 222, Palmerston North, New Zealand 4442

Supporting Information

ABSTRACT: The synthesis and characterization of the fluxional, d^{10} cyclotriphosphazene complexes, $[MLCl_2]$ (M = Zn, Cd, and Hg; L = *spiro*-[(1,1′-biphenyl)-2,2′-dioxy]tetrakis-(4-methyl-2-pyridyloxy)cyclotriphosphazene), are described. Single-crystal X-ray structures show that the zinc complex has crystallized into two crystal forms: one as a tetrahedral species, with a N_2Cl_2 donor set in which a *geminal* pair of the pendant pyridyloxy nitrogen atoms binds to the zinc, and the other as a trigonal-bipyramidal (tbp) one, with an N_3Cl_2 donor set. The third nitrogen atom comes from the phosphazene ring and the two pyridyl ligands are non-*geminal*. The asymmetric unit of the cadmium complex contains three structurally distinct molecules. One molecule has a tbp structure similar to that of the zinc complex. The second molecule has a six-coordinate, distorted octahedral geometry around the cadmium center with a N_4Cl_2 donor set, with three of the nitrogen donor atoms coming from the pendant pyridyloxy arms. The third site contains a tbp complex and a distorted octahedral species with a relative occupancy of 3:1. The identification of these three different forms in the one crystal suggests that the energy difference between the tbp and distorted octahedral isomers is not large. Quantitative analysis of the ^{1}H NMR and variable-temperature ^{31}P NMR spectra of the zinc, cadmium, and mercury complexes in a CD_2Cl_2 solution, coupled with the X-ray structural results, shows that an associative fluxional mechanism ($\Delta S^{\ddagger} < -65$ J mol^{-1} K^{-1}) is operating.

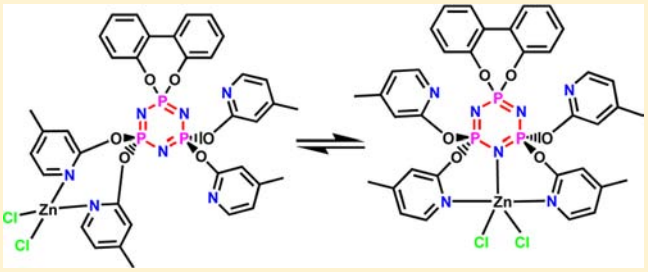

INTRODUCTION

Phosphazenes encompass a remarkable range of compounds containing phosphorus and nitrogen atoms linked to form polymeric chains, oligomers, or cyclic species, with the general formula $[NPR_2]_n$.[1,2] The pendant R groups, which are attached to the phosphorus atoms of the PN backbone, can be readily varied to allow tailoring of the properties of the phosphazenes to achieve the desired outcomes. Although much current research is focused on the synthesis, properties, and potential applications of polyphosphazenes, the synthesis and characterization of small-molecule cyclotriphosphazenes, cyclotetraphosphazenes, and higher homologues have played an essential role in the development and understanding of the polymer systems. This is particularly true for metallo-substituted polyphosphazenes in which the pendant R group contains a donor function to enable it to bind to metals.[3,4]

Previously, we and others have reported the coordination chemistry of hexakis(2-pyridyloxy)cyclotriphosphazene and hexakis(4-methyl-2-pyridyloxy)cyclotriphosphazene and have shown that they are versatile multimodal ligands that display a range of binding modes, often unpredictable, as a result of the flexibility of the phenoxy hinge linking the pyridyl group to the phosphazene ring phosphorus atoms.[5−9] Density functional theory (DFT) calculations have shown that divalent metal ions bind to the phosphazene ring nitrogen atom via a σ-type bond along with a transfer of some electron density from P−N bonds to the metal 4s orbital.[10] We have also reported that replacing sets of *geminal* 2-pyridyloxy groups with spirocyclic 2,2′-dioxybiphenyl groups enables better control of the coordination behavior of these cyclotriphosphazene ligands.[11] In this latter study, it was observed that the five-coordinate, trigonal-bipyramidal (tbp) complexes, e.g., $[CoLX_2]$ [L = (2,2′-dioxybiphenyl)tetrakis(4-methyl-2-pyridyloxy)-cyclotriphosphazene; X = Cl and Br], underwent a structural rearrangement in solution to yield tetrahedral (tet) complexes. To gain further insight into the solution behavior of such complexes including possible fluxionality, the diamagnetic d^{10} complexes $[ZnLCl_2]$, $[CdLCl_2]$, and $[HgLCl_2]$ have been studied.

Studies on the fluxional behavior of complexes containing the cyclotriphosphazene ring are limited. The first reported study was on a square-planar $PdCl_2$ complex with tetrakis(3,5-dimethylpyrazolyl)cyclotriphosphazene, which had one ring phosphorus blocked by noncoordinating groups.[12] A coordination and conformation change (from a non-*geminal* N_2 boat to a *geminal* N_2 chair) was detected in solution by NMR. A more comprehensive study by Byun et al. on mono- and dinuclear d^{10} metal ions with hexakis(3,5-dimethylpyrazolyl)-cyclotriphosphazene showed that the dynamic behavior in

Received: June 25, 2012
Published: October 1, 2012

   dx.doi.org/10.1021/ic3013574 | *Inorg. Chem.* 2012, 51, 10884−10892

solution was complex, sometimes with more than one species being present.[13] From the NMR spectra of the adducts of $P_3N_3Cl_6$ with aluminum and gallium trichlorides, it was suggested that in each case the observed fluxional process was due to dissociation and recombination of the Lewis acids.[14] However, in a recent more detailed study, it was concluded that for the complexes $[(P_3N_3Cl_6)MX_3]$ (M = Al and Ga; X = halide) the exchange is taking place via a process in which free MX_3 is not generated.[15] In the case of a mixed-metal lithium–aluminum phosphazenate, the NMR spectrum was interpreted in terms of the three-coordinated lithium ions oscillating between mono- and bidentate coordination.[16] All of the reports propose mechanisms that are consistent with NMR data, and where crystal structures have been obtained, it is implied that the low-temperature solution structure is closest to that of the X-ray structure. For the present study, the ligand L (Chart 1)

Chart 1. Ligand L

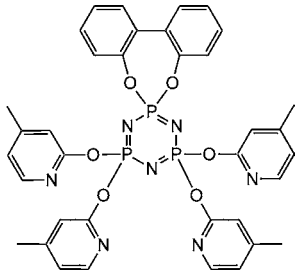

was designed to provide a nitrogen-rich environment for coordination to the d^{10} metal ions via electron donation from 4-methyl-2-pyridyloxy moieties and the phosphazene ring nitrogen atom. In addition, this ligand conferred good solubility and ready assignment of the ^1H NMR signal of the proton ortho to the pyridyl nitrogen atom. The use of the blocking biphenolato group on the phosphazene ring was expected to effectively constrain the coordination site and reduce the complexity of the variable-temperature spectra.

EXPERIMENTAL SECTION

General Procedures. All manipulations were carried out under nitrogen using standard Schlenk techniques. Analytical-grade solvents were purchased from standard chemical suppliers and used without further purification. Hexachlorocyclotriphosphazene (Otsuka Chemical Co. Ltd.), 2-hydroxy-4-methylpyridine (Aldrich), $ZnCl_2{\cdot}xH_2O$ (May and Baker), and $HgCl_2$ (May and Baker) were used as received, and $CdCl_2{\cdot}2.5H_2O$ (Hopkin and Williams) was dried at 140 °C prior to use. The synthesis of the ligand L was as previously described.[11] Microanalyses were performed by Campbell Microanalytical Laboratory, University of Otago. Variable-temperature NMR spectra were recorded on a Bruker Avance 400 MHz spectrometer in CD_2Cl_2; temperature calibration was performed using 4% methanol in methanol-d_4 with a trace of HCl.[17] Line-shape analysis was performed using the program *SpinWorks*.[18] Electrospray mass spectrometry (ESMS) spectra were collected from MeCN solutions on a Micromass ZMD spectrometer run in positive-ion mode.

Syntheses. *tbp-[ZnLCl$_2$] and tet-[ZnLCl$_2$].* A mixture of L (0.101 g, 0.134 mmol) and $ZnCl_2$ (0.018 g, 0.132 mmol) was stirred overnight in 30 mL of CH_2Cl_2. The resulting cloudy solution was filtered through Celite and then taken to dryness to give a white solid. After washing with hexane, the solid was dried at 70 °C under vacuum overnight and used for analysis. Anal. Calcd for $C_{36}H_{32}Cl_2N_7O_6P_3Zn{\cdot}0.33C_6H_{14}$ (917.97): C, 49.72; H, 4.17; N, 10.68. Found: C, 49.51; H, 3.96; N, 10.68. $^{31}P\{^1H\}$ NMR ($CDCl_3$): δ 22.08 (t, J = 102.8 Hz), 7.76 (d, J = 100.9 Hz). ^1H NMR ($CDCl_3$): δ 8.32 (d, J = 5.0 Hz), 7.10 (d, J = 5.0 Hz), 6.93 (s), 2.37 (s, CH_3). ESMS: m/z 850 ($[ZnLCl]^+$). Layering hexane over a concentrated solution of the above product dissolved in CH_2Cl_2 afforded X-ray-quality crystals, identified as tbp-$[ZnLCl_2]{\cdot}CH_2Cl_2$. X-ray-quality crystals of a second form, tet-$[ZnLCl_2]{\cdot}2.5CH_2Cl_2$, were obtained by dissolving the remaining solid that was left in the reaction flask in excess CH_2Cl_2 and layering with hexane.

[CdLCl$_2$]. A mixture of L (0.139 g, 0.180 mmol) and $CdCl_2$ (0.034 g, 0.180 mmol) was stirred overnight in 60 mL of CH_2Cl_2. The cloudy solution was filtered through Celite with CH_2Cl_2. The solution was reduced to approximately 10 mL and a layer of hexane added. Upon standing, X-ray-quality crystals formed (0.144 g, 82%), which were

Table 1. Crystal and Refinement Data for the Complexes

	tet-$[ZnLCl_2]{\cdot}2.5CH_2Cl_2$	tbp-$[ZnLCl_2]{\cdot}CH_2Cl_2$	3$[CdLCl_2]{\cdot}2.75CH_2Cl_2{\cdot}0.25H_2O{\cdot}0.375C_6H_{14}$
molecular formula	$C_{38.5}H_{37}Cl_5N_7O_6P_3Zn$	$C_{37}H_{34}Cl_4N_7O_6P_3Zn$	$C_{37.67}H_{35.75}CdCl_{3.83}N_7O_{6.08}P_3$
mol wt	1100.18	972.79	1025.02
T (K)	97(2)	98(2)	93(2)
cryst syst	triclinic	monoclinic	triclinic
space group	$P\bar{1}$	$P2(1)/c$	$P\bar{1}$
a (Å)	14.6984(10)	17.512(4)	13.8423(5)
b (Å)	16.7607(11)	15.990(3)	17.6519(7)
c (Å)	21.9219(15)	14.686(3)	27.6057(11)
α (deg)	97.417(4)	90	90.811(2)
β (deg)	104.210(4)	92.93(3)	94.710(2)
γ (deg)	111.410(4)	90	101.398(2)
V (Å^3)	4728.8(6)	4106.7(14)	6586.7(4)
Z (Z')	4 (2)	4 (1)	2 (3)
μ(Mo Kα) (mm^{-1})	1.069	1.031	0.893
ρ_{calc} (g cm^{-3})	1.545	1.573	1.550
$2\theta_{max}$ (deg)	50.70	62.46	50.16
no. of unique reflns	17242	7017	22601
data/restraints/param	17242/21/1152	7017/42/543	22565/745/1692
final R indices [$I > 2\sigma(I)$]	R1 = 0.0680, wR2 = 0.1716	R1 = 0.0572, wR2 = 0.1506	R1 = 0.0594, wR2 = 0.1025
R indices (all data)	R1 = 0.1366, wR2 = 0.2243	R1 = 0.0724, wR2 = 0.1642	R1 = 0.0914, wR2 = 0.1128
GOF on F^2	1.045	1.032	1.068

dx.doi.org/10.1021/ic3013574 | *Inorg. Chem.* 2012, 51, 10884–10892

then dried overnight under vacuum at 70 °C for analysis. Anal. Caldd for $C_{36}H_{32}CdCl_2N_7O_6P_3$ (934.92): C, 46.25; H, 3.45; N, 10.49; Cl, 7.58. Found: C, 46.48; H, 3.52; N,10.41; Cl, 7.59. $^{31}P\{^1H\}$ NMR ($CDCl_3$): δ 23.03 (t, J = 100.9 Hz), 6.52 (d, J = 103.3 Hz). ^1H NMR ($CDCl_3$): δ 8.25 (d, J = 5.2 Hz), 7.01 (d, J = 5.1 Hz), 6.86 (s), 2.35 (s, methyl). ESMS: m/z 900 ($[CdLCl]^+$).

[HgLCl$_2$]. A mixture of L (0.110 g, 0.146 mmol) and $HgCl_2$ (0.036 g, 0.132 mmol) was stirred overnight in 30 mL of CH_2Cl_2. The cloudy white solution was filtered through Celite with 30 mL of CH_2Cl_2. After the resulting solution was reduced to approximately 10 mL, a layer of hexane was added. Nucleation produced a white powder (0.07 g, 49%), which was dried overnight at 70 °C under vacuum and used for analysis. Anal. Calcd for $C_{36}H_{32}Cl_2HgN_7O_6P_3{\cdot}0.5C_6H_{14}$ (1067.20): C, 43.89; H, 3.78; N, 9.19. Found: C, 43.60; H, 3.67; N, 9.30. $^{31}P\{^1H\}$ NMR ($CDCl_3$): δ 24.80 (t, J = 97.1 Hz), 7.35 (d, J = 99.3 Hz). ^1H NMR ($CDCl_3$): δ 7.98 (d, J = 5.1 Hz), 6.95 (d, J = 4.9 Hz), 6.88 (s), 2.34 (s, methyl). ESMS: m/z 988 ($[HgLCl]^+$).

Crystallography. X-ray data were collected on a Siemens P4 four-circle diffractometer, using a Siemens SMART 1K CCD area detector. The crystals were mounted in an inert oil, transferred into the cold gas stream of the goniostat, and irradiated with graphite-monochromated Mo Kα (λ = 0.71073 Å) X-rays. The data were collected by the *SMART* program and processed with *SAINT*[19] to apply Lorentz and polarization corrections to the diffraction spots (integrated three-dimensionally). The structures were solved by direct methods and refined using the *SHELXTL* program.[20] Hydrogen atoms were calculated at ideal positions. Although the number of reflections collected for tbp-$[ZnLCl_2]{\cdot}CH_2Cl_2$ was lower than desirable because of a technical fault, the structure has been solved to an acceptable standard. Attempts to grow more crystals resulted in either tet-$[ZnLCl_2]{\cdot}2.5CH_2Cl_2$ or decomposition products. Crystal data are given in Table 1.

RESULTS AND DISCUSSION

Syntheses of the Complexes. The metal complexes were obtained by stirring the appropriate divalent metal chloride with the ligand L in a 1:1 mole ratio dissolved in CH_2Cl_2 until the $^{31}P\{^1H\}$ NMR spectra showed that the reactions were complete. The analytical data, given in the Experimental Section, indicate that the complexes are formed in a 1:1 metal–ligand ratio, although as is typical for aromatic phosphazene-based ligands and their complexes,[21] retention of trapped solvent molecules is evident from the results. Positive-ion ESMS spectra exhibited peaks consistent with formation of the $[MLCl]^+$ cation. For $[ZnLCl_2]$, both tetrahedral and trigonal-bipyramidal isomers were identified in two separate crystal forms by single-crystal X-ray crystallography. By contrast, the cadmium complex, $[CdLCl_2]$, crystallized with three distinct molecules in the unit cell. All of the complexes exhibited good solubility in CH_2Cl_2, and variable-temperature NMR spectral measurements showed them all to be fluxional in this solvent.

X-ray Crystallographic Studies: tet-$[ZnLCl_2]{\cdot}2.5CH_2Cl_2$. The tetrahedral form of the zinc chloride complex, tet-$[ZnLCl_2]{\cdot}2.5CH_2Cl_2$ (depicted in Figure 1 with selected bond lengths and angles given in Table 2), crystallizes in space group $P\bar{1}$ with two distinct molecules of the complex (labeled A and B) and five molecules of CH_2Cl_2 in the asymmetric unit. Both molecules have the zinc ion in the center of a distorted $ZnCl_2N_2$ tetrahedral arrangement, similar to that found in the tetrahedral sites in the pyridyloxy compounds, $[(ZnCl_2)_2L^a]$ [L^a = hexakis(2-pyridyloxy)-cyclotriphosphazene][8] and $[ZnL^bCl_2]$ [L^b = bis(2,2′-dioxybiphenyl)bis(2-pyridyloxy)cyclotriphosphazene][11] as well as in other dipyridinedichlorozinc(II) complexes.[22,23] As in $[(ZnCl_2)_2L^a]$ and $[ZnL^bCl_2]$, the two coordinated pyridyl arms of the phosphazene bound to the zinc in a *geminal* fashion. In

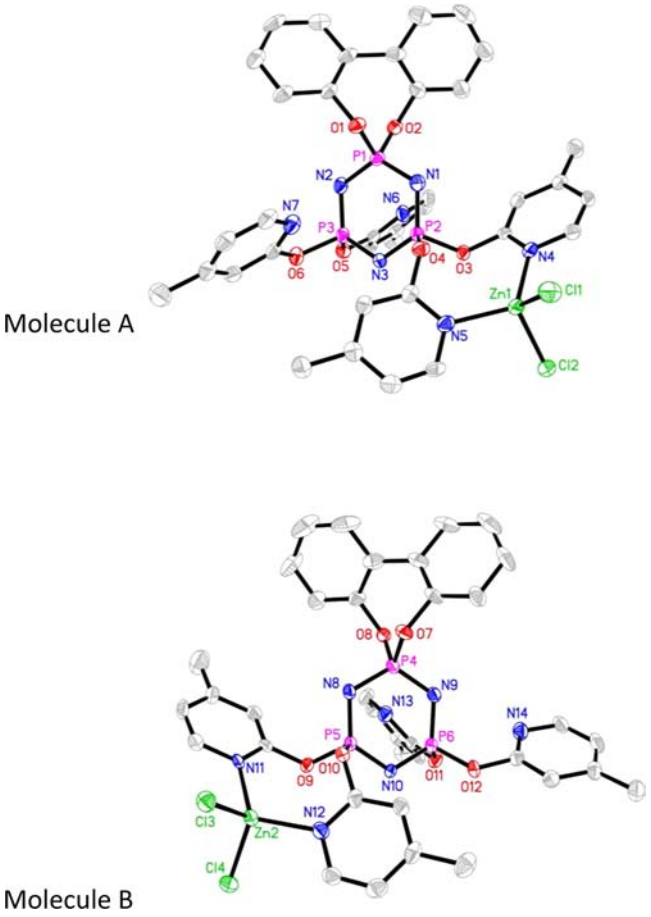

Figure 1. Two molecules of tet-$[ZnLCl_2]$ with hydrogen atoms are removed for clarity. Thermal ellipsoids are drawn at 50% probability.

both molecules, the distances between the noncoordinated pyridyl nitrogen atoms attached to the phosphazene phosphorus atoms P3 (for molecule A, 2.783 and 2.853 Å) and P6 (for molecule B, 2.849 and 2.921 Å) are significantly less than the sum of the van der Waals radii (P···N = 3.35 Å). A similar interaction, characterized also by a near-zero N_{py}–C–O–P torsion angle, was first observed in a bis(2-pyridylthioxy)-substituted cyclotriphosphazene and was ascribed to the host–guest type of interaction.[24,25] Moreover, it has also been seen in a range of 2-pyridyloxy-substituted cyclotriphosphazenes, where, using DFT calculations, the interaction was rationalized in terms of the donation of electron density from the nitrogen lone pair to the cyclophosphazene ring.[26] In molecule A, both of the *geminal* noncoordinated pyridyl rings are approximately normal to the cyclotriphosphazene ring, but in molecule B, one of the rings is twisted away, thus lengthening the P6···N14 distance to 2.921 Å. tet-$[ZnLCl_2]{\cdot}2.5CH_2Cl_2$ has two chiral centers forming intramolecular macrocycles that demonstrate the different directions of rotation in each molecule. There is a seven-membered spiro ring with the biphenolate moiety and an eight-membered spiro ring containing the zinc(II) center. In molecule A, atoms O4 and O3 of the coordinated *geminal* pyridyloxy groups take on a clockwise twist relative to P2 (*R* configuration), whereas in molecule B, the corresponding atoms O9 and O10 display an *S* configuration. Similarly, biphenolato atoms O1 and O2 and atoms O7 and O8 also display *S* and *R* configurations, respectively. That is, the molecules A and B are enantiomers and not diasteroisomers,

dx.doi.org/10.1021/ic3013574 | *Inorg. Chem.* 2012, 51, 10884–10892

Table 2. Selected Bond Lengths (Å) and Angles (deg) for tet-[$ZnLCl_2$]

				$CdLCl_2$			
	tet-$ZnLCl_2$		tpb-$ZnLCl_2$	tbp	oct	0.75tbp	0.25oct
$M-N_{py}$	2.036(5)	2.024(5)	2.265(3)	2.440(5)	2.530(4)	2.484(5)	
$M-N_{py}$	2.050(6)	2.060(6)	2.274(3)	2.493(4)	2.549(4)	2.518(5)	
$M-N_{py}$					2.473(5)		2.427(19)
$M-N_{phz}$			2.056(4)	2.309(4)	2.406(4)	2.318(4)	
M−Cl	2.237(2)	2.240(2)	2.231(1)	2.441(2)	2.468(2)	2.412(4)	2.553(12)
M−Cl	2.248(2)	2.251(2)	2.231(1)	2.459(1)	2.492(1)	2.428(2)	2.586(8)
$N_{py}-M-N_{py}$			175.2(1)	166.5(1)	163.5(1)	163.5(1)	
$N_{py}*-M-N_{py}$	117.4(2)	117.8(2)			87.8(2), 89.0(2)		91.4(6), 94.9(5)
$N_{phz}-M-N_{py}*$					72.6(1)*		76.1(5)
$N_{phz}-M-N_{py}$			87.7(1), 88.1(1)	82.1(1), 86.0(1)	81.3(2), 82.4(2)	81.9(2), 84.9(2)	
$N_{py}*-M-Cl$					85.2(1)*		84.4(6)
$N_{py}-M-Cl$	103.4(2)−110.52(2)	101.7(2)−112.9(2)	90.0(1)−93.7(1)	87.1(1)−98.9(1)	89.6(1)−98.9(1)	87.7(1)−98.4(1)	86.7(3)−98.7(2)
$N_{phz}-M-Cl$			115.7(1), 121.9(1)	120.1(1), 120.8(1)	97.0(1), 157.7(1)	117.5(1), 122.0(1)	102.9(3), 160.5(5)
$N_{py}*-M-Cl$					169.5(1)*		178.0(6)
Cl−M−Cl	113.2(1)	112.5(1)	122.4(1)	118.4(1)	105.3(1)	120.5(1)	96.6(3)
P−N	1.565(5)−1.596(5)	1.564(5)−1.597(5)	1.550(5)−1.579(5)	1.567(4)−1.586(5)	1.575(5)−1.586(5)	1.581(4)−1.592(4)	
P−N(coord)			1.597(5), 1.600(5)	1.606(5)−1.617(4)	1.605(5)−1.616(5)	1.595(4)−1.607(4)	
rmsd (plane)	0.026	0.064	0.066	0.050	0.045	0.057	

dx.doi.org/10.1021/ic3013574 | Inorg. Chem. 2012, 51, 10884−10892

indicating that the *RS* (or *SR*) configuration is energetically favored over the *RR* (or *SS*) configuration.

tbp-[$ZnLCl_2$]·CH_2Cl_2. The trigonal-bipyramidal form of the complex, tbp-[$ZnLCl_2$]·CH_2Cl_2, crystallized in space group $P2(1)/c$ (crystallographic and refinement details in Table 1). The equatorial bonds of the N_3Cl_2 donor set to the zinc(II) center are provided by the phosphazene nitrogen atom (opposite the phosphorus bearing the biphenolato moiety) and two chloro ligands. Axial coordination is provided by two non-*geminal transoid* pyridyl nitrogen-donor atoms, N4 and N6, coordinating in a near-linear manner, with the N4−Zn1−N6 angle being 175.2(1)°. Overall, the structural index, τ,[27] of 0.89 indicates only a slight distortion from the ideal trigonal-bipyramidal symmetry. The equatorial bond length, Zn1−N3 at 2.056(4) Å, is considerably shorter than the axial Zn−N bonds of 2.265(3) and 2.274(3) Å. As in tet-[$ZnLCl_2$], the noncoordinating pyridyl rings are interacting with the cyclotriphosphazene nitrogen atoms [P2···N5 = 2.814 Å and P3···N7 = 2.809 Å], with the torsion angle N−C−O−P again being close to zero. The molecule is depicted in Figure 2, and selected

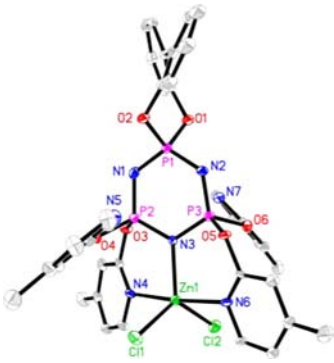

Figure 2. Structure of tbp-[$ZnLCl_2$] with hydrogen atoms removed for clarity. Thermal ellipsoids are drawn at 50% probability.

bond lengths and angles are given in Table 2. Similar coordination geometries are found in two other 2-pyridyloxy-substituted trigonal-bipyramidal complexes, red-[NiL^aCl_2][8] and the five-coordinate site in [$(ZnCl_2)_2L^a$].[8] By contrast, in the related trigonal-bipyramidal complexes of cobalt(II) and copper(II), the pyridyloxy arms coordinate in a non-*geminal* but *cisoid* fashion.[6,8]

The bond lengths within the phosphazene ring tbp-[$ZnLCl_2$] show the expected trend[3] on coordination of a ring nitrogen atom to a metal ion in that the P−N bonds that flank N3; namely, P2−N3 and P3−N3, tend to be slightly longer [1.600(3) and 1.597(4) Å] than the other ring P−N bonds [1.555(4)−1.579(3) Å]. This is also observed in the cadmium species that have phosphazene ring nitrogen coordination (see below) and can be explained in terms of the electron density being transferred from P−N bonding orbitals to an appropriate outer orbital of the metal ion.[10]

When tet-[$ZnLCl_2$] and tbp-[$ZnLCl_2$] are compared, there is a substantial opening up of the P−O−C_{py} bond angles from around 120−122° for uncoordinated pyridyloxy groups making an optimal interaction with a phosphazene phosphorus atom and zinc-coordinated pyridyloxy groups in tet-[$ZnLCl_2$] to 125−125° in tbp-[$ZnLCl_2$].

3[$CdLCl_2$]·2.75CH_2Cl_2·0.25H_2O·0.375C_6H_{14}. The cadmium complex, which crystallized in space group $P\bar{1}$, has three distinct [$CdLCl_2$] sites in the asymmetric unit: one that accommodates a trigonal-bipyramidal species, like tbp-[$ZnLCl_2$], a second that accommodates an octahedral species, and a third that is a 3:1 disorder of a trigonal-bipyramidal molecule, like tbp-[$ZnLCl_2$], and an octahedral molecule. Space is filled by a mixture of CH_2Cl_2 spread over four sites: one in full occupancy, two in 0.75 occupancy, and one in 0.25 occupancy. Cyclohexane disposed about a center of inversion in 0.375 occupancy (0.75 per cell) and a water molecule in an occupancy of 0.25, with the disorder in solvate species a consequence of the disordered [$CdLCl_2$] molecule moieties. Selected bond distances and angles are given in Table 2. One molecule, tbp-[$CdLCl_2$], has a trigonal-bipyramidal structure similar to that of the zinc analogue, including the non-*geminal transoid* disposition of the pyridyl rings (Figure 3a). The τ value at 0.76 is less than that observed for tbp-[$ZnLCl_2$], indicating a greater distortion from the ideal,[27] as does the deviation of the N18−Cd3−N20 bond angle away from linear to 166.5(7)°. This distortion results from the much larger size of the Cd^{2+} ion compared to the Zn^{2+} ion, which leads to a 0.25-Å lengthening of the metal ion to phosphazene nitrogen bond from 2.056(4) to 2.309(4) Å. Similarly to tbp-[$ZnLCl_2$], this equatorial Cd1−N3 bond distance of 2.309(4) Å is shorter than the axial Cd−N distances to pyridyl nitrogen atoms of 2.440(5) and 2.493(4) Å. The two uncoordinated pyridyl groups again interact with the phosphazene phosphorus atoms [N2···P5 = 2.823 Å and N7···P3 = 2.820 Å].

The second molecule, oct-[$CdLCl_2$], has a six-coordinate, distorted octahedral geometry around the cadmium center (Figure 3b), with a N_4Cl_2 donor set similar to that seen for green-[NiL^aCl_2].[8] Hence, there are two trans Cd−N longer bonds from two non-*geminal transoid* pyridyl nitrogen atoms [Cd3−N18 = 2.530(4) Å and Cd3−N20 = 2.549(4) Å; N18−Cd3−N20 = 163.5(1)°] and two shorter cis Cd−N bonds through N19(pyridyl) and N17(phosphazene) [2.473(5) and 2.406(4) Å]. The *cis*-chloride ions make up the remainder of the donor set. As before, the remaining uncoordinated pyridyl ring nitrogen atom (N21) interacts with a phosphazene ring phosphorus atom (P9···N21 = 2.831 Å).

The third molecule in the unit cell, tbp/oct-[$CdLCl_2$], is disordered (Figure 3c), with the major form being a trigonal-bipyramidal complex (occupancy 0.75) and the minor form being a distorted octahedral species (occupancy 0.25). One pyridyloxy arm is either coordinated to the cadmium [Cd2−N14A = 2.427(19) Å] to give a distorted octahedral structure very similar to oct-[$CdLCl_2$] or twisted away from the metal center to lie over the phosphazene ring to interact weakly with a ring phosphorus atom [P6···N14 = 2.817 Å], hence giving rise to a trigonal-bipyramidal structure very similar to that for tbp-[$CdLCl_2$]. The bond parameters for the two species (Table 2) are similar to those found for the separate tbp-[$CdLCl_2$] and oct-[$CdLCl_2$] molecules in the crystal. The identification of these three different forms in the one crystal suggests that the energy difference between the trigonal-bipyramidal and distorted octahedral isomers is not large and that in solution the molecule would exhibit fluxionality.

Variable-Temperature (VT) NMR Studies. The use of the (4-methyl-2-pyridyloxy)cyclotriphosphazene ligand, L, allows the assignment of proton signals for VT ^1H NMR studies. For each complex, there are four ortho protons H3 (Chart 2) to be considered. In the solid state, either two or three are coordinated, with the remainder remaining free. However, in a CD_2Cl_2 solution at 298 K, these protons become equivalent,

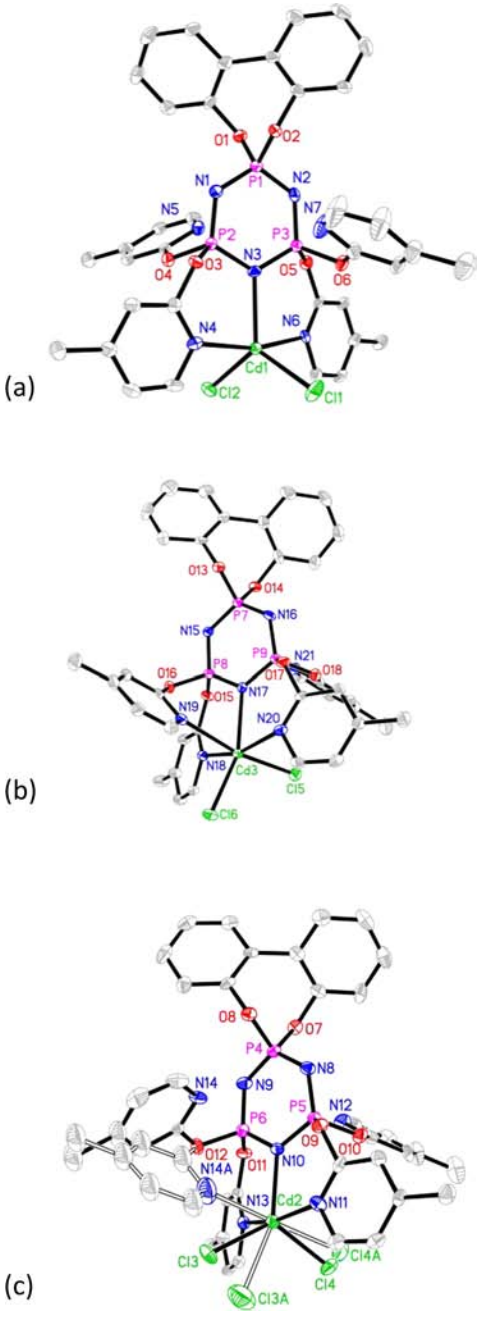

Figure 3. Three different molecules of $[CdLCl_2]$ with hydrogen atoms removed for clarity: (a) tbp-$[CdLCl_2]$; (b) oct-$[CdLCl_2]$; (c) tbp/oct-$[CdLCl_2]$.

Chart 2. Hydrogen Atom Numbering on the Pyridyloxy Moiety

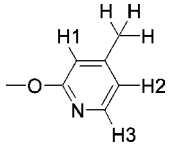

appearing at ~8 ppm ($J \approx 5$ Hz) as a doublet, because of coupling with the meta hydrogen atom H2.

As the temperature is decreased for $[CdLCl_2]$ (Figure 4) and also for $[HgLCl_2]$ (Figure S1 in the Supporting Information), this signal coalesces into a singlet at ~250 K (T_c) that then

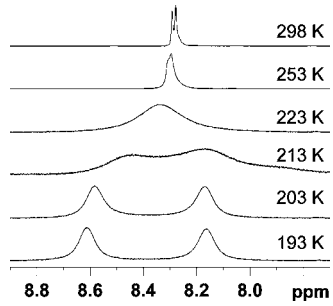

Figure 4. VT ^{1}H NMR spectra for proton H3 of $[CdLCl_2]$ in CD_2Cl_2.

broadens before splitting into two broad resonances below 213 K (Cd, δ 8.6, 8.1; Hg, δ 7.8, 7.6).

The broadness of the peaks below T_c for the cadmium and mercury complexes indicates that the fluxional behavior is still occurring because in the static state it would be expected that, as the rate decreased to a point where the magnetic environments of the two ortho hydrogen atoms were inequivalent, the broad singlet signals would once again show coupling to the meta hydrogen atoms and resolve into two well-defined doublets. Unfortunately, the low-temperature limit imposed by the freezing point of CD_2Cl_2 (176 K), prevented spectra from being recorded at lower temperatures, and the complexes decomposed in other possible solvents. For the $[ZnLCl_2]$ complex, a different behavior is observed. Below T_c, the broad resonance of H3 splits to form an asymmetric peak, which subsequently resolves into four broad peaks below 203 K, with a weak fifth signal at approximately 7.95 ppm (Figure 5). The temperature-dependent behavior is fully reversible in that no difference in behavior is observed whether the solutions are being cooled or warmed to a specific temperature.

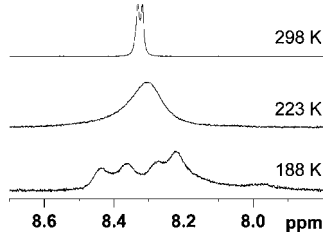

Figure 5. VT ^{1}H NMR spectra for proton H3 of $[ZnLCl_2]$ in CD_2Cl_2.

Experimental and calculated line shapes for the ^{1}H NMR spectra are shown in Figure 6 for $[CdLCl_2]$. For $[CdLCl_2]$ and also for $[HgLCl_2]$, best fits were achieved assuming an ABCD system, where A and B represent the ortho and meta H3 and H2 protons on a *geminal* pyridyloxy group that undergo mutual exchange with another pair, C and D situated in a differing chemical environment. On the basis of the rate data obtained from the line-shape fitting, Arrhenius and Eyring plots could be

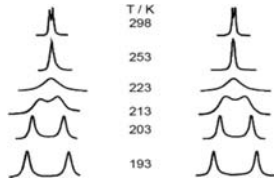

Figure 6. Experimental (left) and calculated (right) ^{1}H line shapes for H3 of $[CdLCl_2]$ in CD_2Cl_2.

dx.doi.org/10.1021/ic3013574 | *Inorg. Chem.* 2012, 51, 10884−10892

obtained (Figures S2–S5 in the Supporting Information), and kinetic data are tabulated in Table 3. Because of its greater

Table 3. Activation Parameters for $[CdLCl_2]$ and $[HgLCl_2]$ in CD_2Cl_2

$[CdLCl_2]$			$[HgLCl_2]$		
T/K	$\Delta G^{\ddagger}$/kJ mol^{-1}	E_a/kJ mol^{-1}	T/K	$\Delta G^{\ddagger}$/kJ mol^{-1}	E_a/kJ mol^{-1}
297	46.5(8)	28.2(5)	297	50.2(8)	23.0(4)
246	41.4(7)		281	48.0(8)	
$[CdLCl_2]$			$[HgLCl_2]$		
T/K	$\Delta G^{\ddagger}$/kJ mol^{-1}	$\Delta H^{\ddagger}$/kJ mol^{-1}	T/K	$\Delta G^{\ddagger}$/kJ mol^{-1}	$\Delta H^{\ddagger}$/kJ mol^{-1}
225	40.5(7)	26.2(4)	246	44.0(7)	21.1(4)
215	40.1(7)		236	43.1(7)	
205	39.8(7)		225	42.0(7)	
$[CdLCl_2]$			$[HgLCl_2]$		
T/K	$\Delta G^{\ddagger}$/kJ mol^{-1}	$\Delta S^{\ddagger}$/J mol^{-1} K^{-1}	T/K	$\Delta G^{\ddagger}$/kJ mol^{-1}	$\Delta S^{\ddagger}$/J mol^{-1} K^{-1}
187	38.7(6)	−65.5(11)	215	41.6(7)	−95.4(16)
			205	40.9(7)	

complexity, accurate modeling of the $[ZnLCl_2]$ system at the low-temperature limit was not possible. If a five-coordinate minor species does exist as indicated by the weak fifth signal at 7.95 ppm in Figure 5, then it can be surmised that this is one of two broad resonances, the second of which may lie beneath the four-peak pattern.

As far as we are aware, kinetic data for fluxional cyclotriphosphazenes are limited to the one study by Tessier et al. on group 13 Lewis acid adducts of $P_3N_3Cl_6$.[15] The calculated activation parameters for $[CdLCl_2]$ and $[HgLCl_2]$ are listed in Table 3. The values of E_a, $\Delta H^{\ddagger}$, and $\Delta G^{\ddagger}$ are all lower than those found by Tessier et al. and are consistent with an intramolecular process. A reasonable explanation for the negative value of $\Delta S^{\ddagger}$ would be synchronous rupture and formation of bonds or additional bond formation. This, combined with the lengthening of the $M-N_{phosphazene}$ bonds and a tendency toward equality for the internal ring P–N bonds and toward planarity for the phosphazene ring, indicates a lower energy, more ordered state. The $^{31}P\{^1H\}$ NMR spectra for $[CdLCl_2]$ and $[HgLCl_2]$ exhibit a doublet and triplet at all temperatures (Figure 7) {$[CdLCl_2]$: δ 6.47 (d, 2P), 23.88 (t, P,

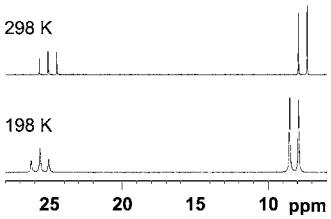

Figure 7. $^{31}P\{^1H\}$ NMR at 298 and 198 K for $[HgLCl_2]$ in CD_2Cl_2.

J_{PP} = 106 Hz. $[HgLCl_2]$: δ 7.57 (d, 2P), 25.06 (t, P, J_{PP} = 99 Hz)}, indicating that there is no change in the chemical environment of the phosphorus atoms upon cooling.

Because solid-state X-ray and low-temperature NMR results are normally in agreement,[28] the NMR spectra for $[CdLCl_2]$ can be rationalized in terms of known solid-state structures reported in this paper. Assuming the trigonal-bipyramidal structure is retained at all temperatures measured, then the fluxional behavior is due to exchange of the pyridyl arms with the metal center. At room temperature, this exchange is sufficiently rapid on the NMR time scale to result in a time-averaged doublet in the ^1H NMR spectrum for the H3 protons, which are ortho to the pyridyl nitrogen atoms. The rate of exchange decreases as the temperature is lowered, and below T_c, equally populated proton environments can be distinguished, as a broad pair of resonances is seen. The crystal structure of the cadmium complex indicates a possible transient octahedral intermediate, viz., oct-$[CdLCl_2]$ (Figure 3b), forming via a species such as tpb/oct-$[CdLCl_2]$ (Figure 3c) for the exchange process that is not visible in either the ^1H or $^{31}P\{^1H\}$ NMR spectra. Although a similar process would be feasible for $[HgLCl_2]$, we were unable to obtain suitable crystals for X-ray structure analysis of this compound.

As for its ^1H NMR, the $[ZnLCl_2]$ complex demonstrates a different behavior at the low-temperature limit (Figure 8). At

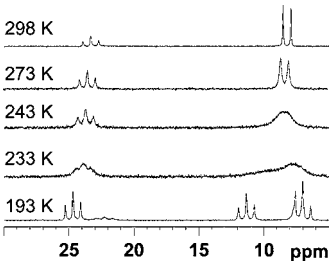

Figure 8. VT $^{31}P\{^1H\}$ NMR for $[ZnLCl_2]$ in CD_2Cl_2.

298 K, the doublet–triplet pattern indicates that two of the three phosphorus atoms are in an equivalent environment. After they coalescence, three triplets are clearly defined at 193 K, with an underlying minor species appearing as a weak triplet–doublet [Major species: δ 6.96 (t), 11.31 (t), 24.65 (t, J_{PP} = 89 Hz). Minor species: δ 7.33 (d), 22.26 (t, J_{PP} = 91 Hz)]. These are shown schematically in Figure 9.

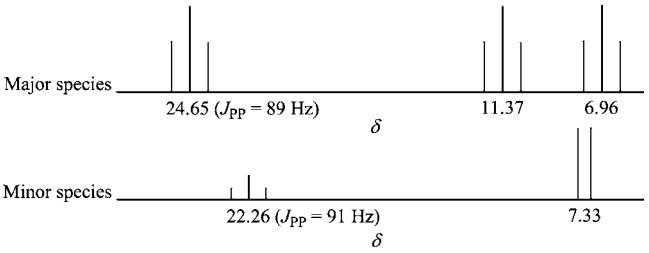

Figure 9. Schematic diagram of the NMR of major and minor species present in the $^{31}P\{^1H\}$ NMR of the $[ZnLCl_2]$ complex at 193 K.

Integrating the triplet pattern at 193 K gave a 1:1:1.7 ratio, which indicates that underlying the triplet at 6.96 ppm there is a second component. A 2D COSY NMR spectrum (Figure S6 in the Supporting Information) at 198 K confirms the underlying doublet coupled to the minor species triplet, suggesting that, for the minor species, two of the phosphorus atoms are magnetically equivalent [δ 7.3 (d), 22.3 (t)].

To eliminate the possibility that the appearance of the minor species at 198 K arises from dissociation of $[ZnLCl_2]$, a small quantity of the free ligand, L, was added to solutions of $[ZnLCl_2]$, $[HgLCl_2]$, and $[CdLCl_2]$ and low-temperature $^{31}P\{^1H\}$ NMR spectra were recorded. The spectra demonstrated that the free ligand is present as a separate species at all

dx.doi.org/10.1021/ic3013574 | Inorg. Chem. 2012, 51, 10884–10892

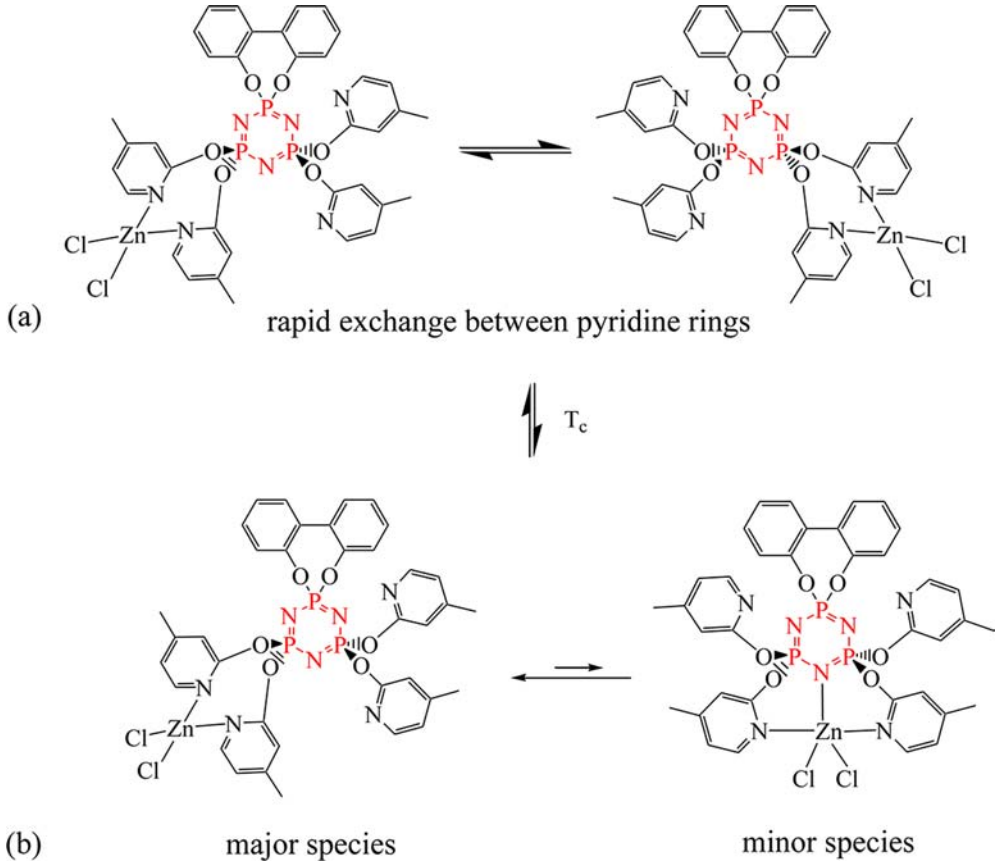

Figure 10. (a) Room temperature configuration with rapid exchange between pyridine rings and (b) possible configurations at low temperature.

temperatures and that the minor species observed is therefore more likely to be due to a nondissociative structural rearrangement in which two of the phosphorus atoms are magnetically equivalent rather than the free ligand. Moreover, the temperature-dependent behavior seen for [$ZnLCl_2$] is reversible, with the minor species doublet−triplet pattern disappearing to leave the three triplets as the temperature is increased.

For [$ZnLCl_2$], by analogy with the solution rearrangement of the [$CoLCl_2$] complex mentioned earlier[11] and with X-ray data that confirm that both trigonal-bipyramidal and tetrahedral structures can exist (Figures 1 and 2), it is argued that in solution at room temperature, the zinc complex forms a tetrahedral structure that undergoes rapid exchange with the pyridine rings (Figure 10) so that the two pyridine-bearing phosphorus atoms appear to be equivalent, giving a time averaged A_2X signal in the VT $^{31}P\{^1H\}$ NMR spectrum. Below T_c, the three observed triplets in the VT $^{31}P\{^1H\}$ NMR spectrum can be viewed as three overlapping doublet of doublets, where the J coupling is such that the signals appear as pseudotriplets. We propose that the required nonequivalence in the phosphorus environments is achieved when the rapid exchange of pyridine pendant arms slows below T_c to a point whereby the tet-[$ZnLCl_2$] structure becomes distinguishable, and all three phosphorus atoms become nonequivalent. With reference to the room temperature NMR spectra, the phosphorus bearing the biphenyldioxy moiety is at lowest field. Tetrahedral coordination around zinc is more likely as typified by tet-[$ZnLCl_2$] (Figure 1) and other 2-pyridyloxy-subsituted cyclophosphazene zinc(II) complexes.[8,11] In the absence of any crystallographic evidence and with the relative rarity of six-coordinate zinc(II) species, we do not favor a mechanism that involves a six-coordinate structure, as demonstrated by oct-[$CdLCl_2$].

In each case, as the low-temperature limit is approached, the five-coordinate structure appears as the underlying doublet−triplet of the minor species. This hypothesis accounts for the observation that the four signals for the ortho proton in the ^1H NMR spectrum arise from four nonequivalent sites, with at the low-temperature limit a fifth signal being part of the five-coordinate environment of the minor species.

■ CONCLUSIONS

The synthesis of the cyclotriphosphazene complexes, [$MLCl_2$] (M = Zn, Cd, and Hg; L = *spiro*-[(1,1′-biphenyl)-2,2′-dioxy]tetrakis(4-methyl-2-pyridyloxy)cyclotriphosphazene), from the group 12 divalent metal chlorides is described. In the solid state, single-crystal X-ray structures show that the zinc complex can be isolated as a tetrahedral isomer, tet-[$ZnLCl_2$], or as a trigonal-bipyramidal one, tbp-[$ZnLCl_2$]. In the latter case, the coordination sphere is completed by a nitrogen atom from the phosphazene ring. Remarkably, the single-crystal X-ray structure of the cadmium(II) analogue contains three crystallographically distinct sites for the complex: one site contains a discrete five-coordinate species, tbp-[$CdLCl_2$], the second a discrete six-coordinate species, oct-[$CdLCl_2$], and the third a 3:1 mixture of tbp-[$CdLCl_2$] and oct-[$CdLCl_2$] that possibly is undergoing dynamic coordinative exchange of a 2-pyridyloxy pendant arm at room temperature. The identification of these three different forms in the one crystal suggests that the energy difference between the trigonal-bipyramidal and distorted octahedral isomers is not large.

dx.doi.org/10.1021/ic3013574 | *Inorg. Chem.* 2012, 51, 10884−10892

VT ^{1}H NMR studies show that all complexes are fluxional in solution. tet-[$ZnLCl_2$] samples alternate *geminal* pyridyl groups, possibly via the trigonal-bipyramidal species, where a phosphazene nitrogen atom coordinates along with a pair of non-*geminal* pyridyl groups (seen in the lowest-temperature ^{31}P NMR spectrum and in one of the X-ray structures). [$CdLCl_2$] and [$HgLCl_2$] behave similarly, with the four pyridyl arms exchanging between coordinated and noncoordinated modes via the unsymmetrical octahedral intermediate observed crystallographically, where three of the four pyridyl rings are coordinated. The calculated activation entropy is strongly negative, supporting the associative mechanism for fluxional behavior proposed from NMR and crystallographic evidence.

■ ASSOCIATED CONTENT

Supporting Information

Crystallographic information in CIF format, Arrhenius and Eyring plots, and spectral data. This material is available free of charge via the Internet at http://pubs.acs.org.

■ AUTHOR INFORMATION

Corresponding Author

*E-mail: e.ainscough@massey.ac.nz (E.W.A.), a.brodie@massey.ac.nz (A.M.B.).

Notes

The authors declare no competing financial interest.

■ ACKNOWLEDGMENTS

We acknowledge financial support, including a postdoctoral fellowship (to C.A.O.) and a Ph.D. scholarship (to S.K.), from the Massey University Research Fund and the RSNZ Marsden Fund (MAU208), respectively. We thank Dr. Jan L. Wikaira (University of Canterbury) for assistance in collecting the X-ray diffraction data and the Otsuka Chemical Co. Ltd. for a gift of hexachlorocyclotriphosphazene.

■ REFERENCES

(1) Allcock, H. R. *Chemistry and Applications of Polyphosphazenes*; Wiley-Interscience: Hoboken, NJ, 2003.

(2) Mark, J. E.; Allcock, H. R.; West, R. *Inorganic Polymers*, 2nd ed.; Oxford University Press: New York, 2005.

(3) Chandrasekhar, V.; Nagendran, S. *Chem. Soc. Rev.* **2001**, *30*, 193−203.

(4) Chandrasekhar, V.; Thilagar, P.; Murugesa Pandian, B. *Coord. Chem. Rev.* **2007**, *251*, 1045−1074.

(5) Ainscough, E. W.; Brodie, A. M.; Depree, C. V. *J. Chem. Soc., Dalton Trans.* **1999**, 4123−4124.

(6) Ainscough, E. W.; Brodie, A. M.; Depree, C. V.; Moubaraki, B.; Murray, K. S.; Otter, C. A. *Dalton Trans.* **2005**, 3337−3343.

(7) Ainscough, E. W.; Brodie, A. M.; Depree, C. V.; Jameson, G. B.; Otter, C. A. *Inorg. Chem.* **2005**, *44*, 7325−7327.

(8) Ainscough, E. W.; Brodie, A. M.; Depree, C. V.; Otter, C. A. *Polyhedron* **2006**, *25*, 2341−2352.

(9) Chandrasekhar, V.; Pandian, B. M.; Azhakar, R. *Inorg. Chem.* **2006**, *45*, 3510−3518.

(10) Davidson, R. J.; Ainscough, E. W.; Brodie, A. M.; Harrison, J. A.; Waterland, M. R. *Eur. J. Inorg. Chem.* **2010**, 1619−1625.

(11) Ainscough, E. W.; Brodie, A. M.; Derwahl, A.; Kirk, S.; Otter, C. A. *Inorg. Chem.* **2007**, *46*, 9841−9852.

(12) Chandrasekaran, A.; Krishnamurthy, S. S.; Nethaji, M. *Inorg. Chem.* **1993**, *32*, 6102−6106.

(13) Byun, Y.; Min, D.; Do, J.; Yun, H.; Do, Y. *Inorg. Chem.* **1996**, *35*, 3981−3989.

(14) Heston, A. J.; Panzner, M. J.; Youngs, W. J.; Tessier, C. A. *Inorg. Chem.* **2005**, *44*, 6518−6520.

(15) Tun, Z.-M.; Heston, A. J.; Panzner, M. J.; Medvetz, D. A.; Wright, B. D.; Savant, D.; Dudipala, V. R.; Banerjee, D.; Rinaldi, P. L.; Youngs, W. J.; Tessier, C. A. *Inorg. Chem.* **2011**, *50*, 8937−8945.

(16) Rivals, F.; Steiner, A. *Eur. J. Inorg. Chem.* **2003**, 3309−3313.

(17) Van Geet, A. L. *Anal. Chem.* **1970**, *42*, 679−680.

(18) Marat, K. *SpinWorks 2.5.1*; University of Manitoba: Winnipeg, Canada, 2006.

(19) *SMART and SAINT, Area Detector Control and Integration Software*; Siemens Analytical X-ray Systems Inc.: Madison, WI, 1996.

(20) Sheldrick, G. M. *SHELXL Suite of Programs for Crystal Structure Analysis*; Institüt für Anorganische Chemie der Universität Göttingen: Göttingen, Germany, 1998.

(21) Horvath, R.; Otter, C. A.; Gordon, K. C.; Brodie, A. M.; Ainscough, E. W. *Inorg. Chem.* **2010**, *49*, 4073−4083.

(22) Steffen, W. L.; Palenik, G. J. *Acta Crystallogr., Sect. B* **1976**, *B32*, 298−300.

(23) Steffen, W. L.; Palenik, G. J. *Inorg. Chem.* **1977**, *16*, 1119−1127.

(24) Jung, O.-S.; Park, S. H.; Lee, Y.-A.; Cho, Y.; Kim, K. M.; Lee, S.-g.; Chae, H. K.; Sohn, Y. S. *Inorg. Chem.* **1996**, *35*, 6899−6901.

(25) Jung, O.-S.; Kim, Y. T.; Lee, H.; Kim, K. M.; Chae, H. K.; Sohn, Y. S. *Bull. Chem. Soc. Jpn.* **1997**, *70*, 2125−2130.

(26) Davidson, R. J. M.Sc. Thesis, Massey University, Palmerston North, New Zealand, 2007.

(27) Addison, A. W.; Rao, T. N.; Reedijk, J.; Van Rijn, J.; Verschoor, G. C. *J. Chem. Soc., Dalton Trans.* **1984**, 1349−1356.

(28) Cotton, F. A.; Wilkinson, G.; Murillo, C. A.; Bochmann, M. *Advanced Inorganic Chemistry*, 6th ed.; Wiley: New York, 1999.